Journal of Oceanology and Limnology

https://doi.org/10.1007/s00343-024-4081-1

Research Paper

Non-targeted metabolomic analysis of *Pyropia yezoensis* metabolites using GC-MS and its regulation under high temperature*

Aurang ZEB[1], Xiuwen YANG[1], Yasmin KHAN[2], Hongyan HE[1], Caiwei FU[1], Dongren ZHANG[1], Jing QU[1], Songdong SHEN[1, **]

[1] *Department of Cell Biology, School of Biology and Basic Medical Sciences, Soochow University, Suzhou 215006, China*

[2] *Department of Biology, School of Life Sciences, Anhui Agricultural University, Hefei 230036, China*

Received Mar. 16, 2024; accepted in principle Apr. 18, 2024; accepted for publication Jun. 3, 2024

Abstract *Pyropia yezoensis* (red algae) or commonly known as nori, is highly regarded for its nutritional benefits and distinct taste, leading to its widespread consumption. The bio-activity and sensory characteristics of *P. yezoensis* are attributed to the metabolites it contains. In this study, identification and quantification of the diverse range of metabolites of *P. yezoensis* and metabolomic analysis were conducted using gas chromatography-mass spectrometry (GC-MS). Furthermore, the impact of high temperature on its metabolites regulation was also investigated. Due to metabolomic analysis, a diverse range of metabolites were identified in *P. yezoensis*, including lipids, amino acids, carbohydrates, and secondary metabolites. Several known bioactive compounds, including alcohol and polyols, amines, amino acids-peptides-analogues, beta hydroxy acids and derivatives, carbohydrates and carbohydrate conjugates, cholestane steroids, dicarboxylic acid and derivatives, and fatty acids and conjugates were detected in abundance, highlighting the nutritional and functional properties of *P. yezoensis*. Additionally, the metabolites composition of *P. yezoensis* was significantly affected in high temperatures, which led to up-regulation of considerable primary metabolites and few were down-regulated, and suggested a potential response and adaptation mechanism of *P. yezoensis* to elevated temperature conditions. This research highlighted the metabolomics of *P. yezoensis*, provided insights into its metabolite composition and regulatory responses to high temperature conditions, enhanced our knowledge of the biochemical pathways and adaptive mechanisms of *P. yezoensis*, which can assist the improvement strategies of utilization and cultivation to promote this valuable alga in response to fluctuating environmental conditions.

Keyword: metabolomics; *Pyropia yezoensis*; metabolite; gas chromatography-mass spectrometry (GC-MS); temperature stress

1 INTRODUCTION

Pyropia yezoensis (Ueda) or nori, formerly known as *Prophyra yezoensis*, is a seaweed of commercial values (Sutherland et al., 2011). The cultivation and harvesting of the gametophyte of *P. yezoensis* is common in East Asia. With an annual production exceeding 1 100 000 t in fresh weight and an estimated annual value of approximately US $1.5 billion, it is a significant seafood resource in this region (http://www.fao.org/fishery/statistics/en). The cultivation of nori production in 2018 was around 1.8 million t, making it the most economically significant marine crops globally (Barange, 2018).

The seaweed commonly utilized for making nori

* Supported by the National Key R&D Program of China (No. 2016YFC1402102), the National Natural Science Foundation of China (No. 41976109), the Ministry of Natural Resources Key Laboratory of Eco-Environmental Science and Technology of China (No. MEEST-2020-2), and the Project Funded by the Priority Academic Program Development of Jiangsu Higher Education Institutions (PAPD)

** Corresponding author: shensongdong@suda.edu.cn

(sushi wrap), *P. yezoensis*, is known for its rich nutritional content. These are extensively consumed for its rich protein, vitamin, and mineral content (Sahoo et al., 2002). It contains 25%–30% protein in dry weight, oligosaccharides that benefits to human health, and some essential vitamins specially vitamin-B12 (Kumar et al., 2021).

Edible marine algae contain a variety of components that may provide health benefits (Niwa, 2010). *P. yezoensis* is known for its protective effects against UV damage and antioxidant properties (Toyosaki and Iwabuchi, 2009; Shin et al., 2011), anticancer (Choi et al., 2015), anti-inflammatory (Eitsuka et al., 2004; Isaka et al., 2015), anti-hypertensive (Hwang et al., 2008), and tissue-healing properties (Mohamed et al., 2012). Multiple research studies have investigated the nutrient composition of fresh *P. yezoensis*. The composition of primary and secondary metabolites has been comprehensively analyzed, including proteins (Noda, 1993), polysaccharide (Zhang et al., 2001; Zhou and Ma, 2006), porphyran (Takahashi et al., 2000; Hirano et al., 2005), vitamins (Miyamoto et al., 2009), and minerals (Qu et al., 2010). Fresh *P. yezoensis* has been found to be rich in proteins, sulfated galactan, choline, taurine, inositol, eicosapentaenoic acid, and minerals such as zinc, copper, manganese, and selenium (Noda, 1993; Qu et al., 2010). The concentrations of free amino acids in *P. yezoensis* blades are significantly influenced by both the genotype of the seaweed and the progression of harvesting (Niwa et al., 2003, 2008).

However, there is currently limited information available on how temperature affects the nutrient composition of *P. yezoensis*. High temperatures have the potential to disrupt the essential enzymes involved in protein synthesis, photosynthesis and respiration leading to adverse effects on plant growth and development (Larcher, 2003). As a result, plants have developed mechanisms to sense their surroundings and adapt through cellular, developmental, and physiological alterations for the enhancement of reproduction and growth practices.

Several studies in proteomics, physiological and genome level analysis have been conducted on the impact of temperature on *Pyropia*. Kayama et al. (1985) revealed that the fatty acid composition of *Pyropia* could be influenced by water temperature. Choi et al. (2013) found that under high temperature conditions, the heat shock protein family of *Pyropia tenera* was primarily produced from its transcripts. Xu et al. (2014) studied the comparative proteomic analysis of *Pyropia haitanensis* under high-temperature stress using liquid chromatography tandem mass spectrometry, and their database searching indicated the response of algal blades to high-temperature stress. They found that nonessential metabolic processes and activities of photosynthesis were reduced in high temperature.

In this study, the alterations in nutrient composition of *P. yezoensis* due to high-temperature conditions were comprehensively analyzed through the application of a gas chromatography-mass spectrometry- (GC-MS-) based metabolomics strategy in conjunction with multivariate data analysis. The focus of this research was to investigate the nutrient composition of *P. yezoensis*, impact of temperature on these nutrients, and regulation of various metabolites in response to different temperature exposures in detail.

2 MATERIAL AND METHOD

2.1 Chemical and instrument

The chemicals used in this study were methanol (Fisher), water, L-2-chlorophenylalanine (Shanghai Hengchuang Biotech), n-hexane (CNW), pyridine (aladdin), chloroform (Greagent), BSTFA (TCI), O-methylhydroxylamine hydrochloride (97%) (Macklin), methyl caprylate standard (Dr. Ehrenstorfeh), methyl nonanoate (C9:0) standard (NU-chek), methyl caprate (C10:0) standard (NU-chek), methyl dodecanoate/methyl laurate (C12:0) standard (NU-chek), methyl tetradecanoate/methyl myristate (C14:0) standard (NU-chek), methyl cetanoate/methyl palmitate (C16:0) standard (Dr. Ehrenstorfeh), methyl octadecanoate/methyl stearate (C18:0) standard (NU-chek), methyl eicosanoate/methyl arachidonate (C20:0) standard (NU-chek), methyl dosenoate/methyl behenate (C22:0) standard (NU-chek), and methyl eicotetradecanoate/methyl lignoate (C24:0) standard (NU-chek). The instruments included electronic balances (Shanghai Yueping Scientific Instrument Co., Ltd.), ultrasonic cleaner (Shenzhen Fuyang Technology Group Co., Ltd.), vortex oscillator (Shanghai Hannuo Instrument Co., Ltd.), fully automatic sample grinder (Shanghai Wanbai Biotechnology Co., Ltd.), freeze concentration centrifugal dryer (Taicang Huamei Biochemical Instrument Factory), high-speed refrigerated centrifuge (Shanghai Lu Xiangyi Instrument Co., Ltd.), gas bath thermostatic shaker (Shanghai Lichen Bangxi Instrument Technology Co., Ltd.), vacuum drying oven (Shanghai Huitai Co., Ltd.), GC-MS (Agilent), and columns (Agilent).

2.2 *Pyropia yezoensis* sample

Samples of *P. yezoensis* were collected in Jianggang cultivating farm located near the shores of the Yellow Sea (33.31°N, 120.78°E) in Jiangsu, China, and transported using container of 4 °C in 5 h to the laboratory. The seaweed thalli were rinsed in cold freshwater to remove any visible contaminants. The thalli of *P. yezoensis* were randomly selected in batches of 20 thalli, with 12 replicates, and washed with mixtures of ethanol (40%–50%) and sodium hypochlorite (1%) to remove epiphytic microbiota (Kientz et al., 2011) prior to GC-MS for metabolomic analysis. The samples were cultured in autoclaved seawater at low 5 °C (6 samples) and high 25 °C (6 samples) for 10 d in 12-h∶12-h day∶light scheme, supplemented with half strength PES (Provasoli's enrichment solution) medium. After 10 d, the samples were harvested and stored at -80 °C by quickly freezing them in liquid nitrogen for GC-MS analysis.

2.3 Sample preparation

GC-MS technique was used for the analysis of metabolomic profiles of *P. yezoensis* extracts in order to assess its metabolic status in response to temperature alterations during culture. Twelve samples, consisting of six from low temperature (LT) 5 °C and six from high temperature (HT) 25 °C, were chosen for the generation of calibration curves and for the purpose of QC (control quality). Samples were air-dried first, ground into powder, and then each sample of about 60 mg was transferred into individual 1.5-mL centrifuge tubes. Two small steel balls (7 mm) were added to each tube, and then methanol-water solution of 600 μL (with a volume ratio of 7∶3) were added. This methanol-water solution contained 4-μg/mL concentration of L-2-chlorophenylalanine. After adding the methanol-water solution and steel balls, the samples were kept at -40 °C for 120 s before being ground for 2 min at 60 Hz. Subsequently, chloroform concentration of about 120 μL was added to each sample, and the samples were vigorously vortexed. After vortex, these samples were subjected to ultrasound-assisted extraction for 10 min at room temperature and kept for 10 min at 4 °C. The samples were centrifuged at 12 000 r/min at 4 °C for 10 min. The aliquots of all samples were pooled together for the preparation of quality control (QC) sample. 150-μL supernatants were transferred from each aliquot to sampling glass vial and finally, at room temperature, the vials were vacuum-dried. After vacuum drying, methoxylamine hydrochloride of 80 μL (dissolved in pyridine at a concentration of 15 mg/mL) was added to vials. Then, the mixture was vortexed vigorously for 2 min and incubated at 37 °C for 60 min. At last, a volume of 50 μL of N, O-bis(trimethylsilyl)trifluoroacetamide (BSTFA) containing 1% trimethylchlorosilane (TMCS) and 20 μL of n-hexane were added to the mixture. Then, 10 internal standards (C8/C9/C10/C12/C14/C16/C18/C20/C22/C24, all chloroform configurations) were added, vortexed for 2 min and derivatized at 70 °C for 60 min. Finally, all the samples were equilibrated at room temperature for 30 min prior to GC-MS analysis.

2.4 GC-MS analysis

2.4.1 Chromatographic and mass spectrometry conditions

A DB-5MS capillary column (Agilent) in dimension of 30 m×0.25 mm×0.25 μm was utilized for GC-MS analysis. The high purity of 99.999% helium gas (carrier gas) was employed at flow rate of 1.0 mL/min. The inlet temperature for the column was set at 260 °C and the injection volume was 1 μL with no splitting with a solvent delay of 6.2 min. The column heater started and maintained for 0.5 min at 60 °C, followed by gain in the temperature to 125 °C at 8 °C/min. The temperature was then raised to 210 °C at the same rate of 8 °C/min, followed by a further increase at 15 °C/min to 270 °C. Finally, the temperature rose at 20 °C/min to extent up to 305 °C and kept for 5 min. The electron bombardment ion source (EI) was operated at 230 °C, while the temperature of quadrupole was maintained at 150 °C. The electron energy was set at 70 eV. The instrument performed quality analysis by scanning a range of m/z 50–500 having mode of full scan (SCAN) (Zhao et al., 2019).

2.4.2 GC-MS and statistical analysis

After pre-treatment of samples completion, the samples were sent to Shanghai (OE Biotech. Co., Ltd.) in Shanghai, China, for comprehensive GC-MS analysis. Metabolite content was determined by calculating the peak area of the metabolites relative to the peak area of the internal standard on the same chromatograph. The sustained data was in the form of log2 transformation using Microsoft Excel. After that, the data matrix was imported for analysis into software SIMCA-P (Version 14.0; Umetrics; Umea; Sweden) (Wheelock and Wheelock, 2013). The

metabolic differences were evaluated using principal component analysis (PCA) and (orthogonal) partial least-squares-discriminant analysis (OPLS-DA) between the LT and HT groups after mean centering and unit variance scaling. In the analysis, the interpretation of ellipse modeled variance represented as Hotelling's T2 with a 95% confidence interval (Aliferis et al., 2013). The models' quality was assessed using R2 and Q2 values, where R2 quantifies the variation elucidated by the model, while Q2 evaluates the model's predictive capability for new data (Mastrangelo et al., 2015). The transformed raw data of *Pyropia yezoensis* metabolites heat map illustrating the *z*-score was constructed using statistical computing of R environment (http://www.r-project.org/). The color scheme of the heat map, generated using ggplot2 in R, signifies the *z*-score for the metabolites (Park et al., 2018). In the context of each variable OPLS-DA modeling, the statistics of VIP (Variable Importance in Projection) were used to assess the overall contribution. Variables meeting the criteria of $P<0.05$ and VIP> 1.0 were deemed significant and relevant for discriminating between groups. Furthermore, the regulated metabolites pathways were further identified according to KEGG, (http://www.genome.jp/kegg/) (Kanehisa and Goto, 2000).

2.5 Metabolic pathway enrichment analysis

The investigation of metabolic pathway modifications in the differential samples was carried out using pathway enrichment analysis of differential metabolites. The pathway enrichment analysis was executed utilizing the KEGG ID of the differential metabolites using KEGG database, allowing us to obtain the results of the metabolic pathway enrichment. To identify pathway entries that showed a significant enrichment in the differentially expressed metabolites relative to the background, hypergeometric tests were used and calculated as:

$$P = 1 - \sum_{i=0}^{m-1} \frac{\begin{bmatrix} M \\ i \end{bmatrix} \begin{bmatrix} N-M \\ n-i \end{bmatrix}}{\begin{bmatrix} N \\ n \end{bmatrix}},$$

N represents the total number of metabolites, with n denoting the number of differentially expressed metabolites within N. Additionally, the metabolites numbers annotated to a specific pathway were represented by M, while m reflects the number of differential metabolites associated to that pathway. By setting a threshold of $P \leq 0.05$, the pathways meeting this criterion were deemed significantly enriched in the differential metabolites. A lower P value suggests a more notable difference in the enrichment of the metabolic pathway.

3 RESULT

3.1 Metabolic profiling of *P. yezoensis*

The effect of temperature on metabolite regulation in *P. yezoensis* was investigated by conducting an analysis of comparing two groups of cultures at significantly different temperatures, HT (high temperature, 25 °C) and LT (low temperature, 5 °C). The intensities of compound peaks in the total ion chromatography (TIC) plot, derived from GC-MS analyses, exhibited significant differences between HT and LT conditions. A total of 283 metabolite peaks were identified, with a majority of these metabolites being linked to primary metabolism (Supplementary Table S1). This observation suggests that the detected metabolites may provide insights into the physiological status of *P. yezoensis*. The metabolites were represented through Average RI, Quant mass, HMDB, METLIN, Lipidmaps, PubChem, kegg, CAS, and inchikey (Fig.1; Supplementary Table S2). These metabolites were classified as Pie-Class, Pie-Subclass, and Pie-Superclass.

The total number of 283 metabolites found in Pie-Class were benzene and substituted derivatives, carboxylic acids and derivatives, fatty acyls, hydroxy

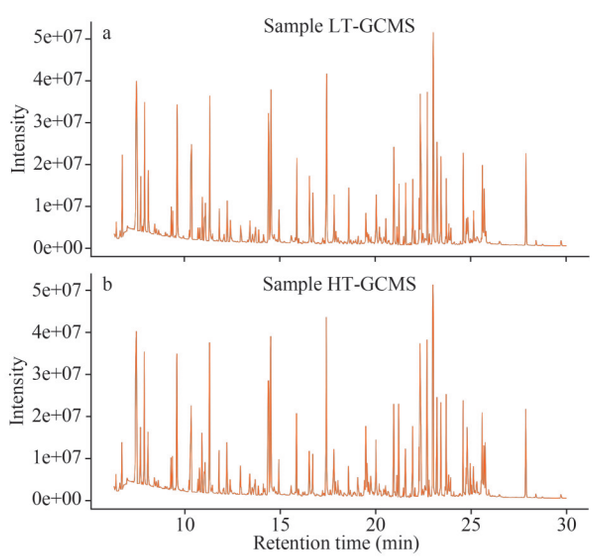

Fig.1 Total ion chromatography (TIC)

a. low temperature samples; b. high temperature samples. The intensities of compound peaks in the total ion chromatography (TIC) obtained from GC-MS analyses.

acids and derivatives, organonitrogen compounds, organooxygen compounds, pyridines and derivatives, steroids and steroid derivatives, unclassified, and others with a number of 4, 50, 43, 11, 7, 74, 5, 5, 33, 51 and percentage of 1.41%, 17.67%, 15.19%, 3.89%, 2.47%, 26.15%, 1.77%, 1.77%, 11.66%, 18.02%, respectively.

In Pie-Subclass there were alcohol and polyols, amines, amino acids-peptides-analogues, beta hydroxy acids and derivatives, Carbohydrates and carbohydrate conjugates conjugates, cholestane steroids, dicarboxylic acid and derivatives, Fatty acids and conjugates, unclassified, and others with number of 12, 7, 39, 5, 62, 4, 8, 33, 44, 69, and percentage of 4.24%, 2.47%, 13.78%, 1.77%, 21.91%, 1.41%, 2.83%, 11.66%, 15.55%, 24.38%, respectively.

The representation in Pie-Superclass were benzenoids, lipids and lipid-like molecules, Nucleosides, nucleotides, and analogues, organic acid and derivatives, organic nitrogen compounds, organic oxygen compounds, organoheterocyclic compounds, phenylpropanoids and polyketides, unclassified, others with number of 7, 58, 7, 70, 7, 74, 18, 4, 33, 5, and percentage of 2.47%, 20.49%, 2.47%, 24.73%, 2.47%, 26.15%, 6.36%, 1.41%, 11.66%, 1.77%, respectively (Fig.2).

3.2 Multivariate statistical analysis of the GC-MS data

The relative intensities of the 81 metabolite peaks were standardized using internal standards and then used for multivariate statistical analyses. First, PCA with unsupervised pattern recognition was conducted to generate an overview of the metabolic patterns within the six samples from each group. The analysis revealed that LT and HT samples were distinctly separated into different groups on the first two principal components, with no outliers identified. Additionally, PCA plots were created to further examine the similarities and differences between the LT and HT samples at each time point (Fig.3a).

In addition, we employed OPLS-DA to provide a more precise evaluation of the metabolic patterns in these samples. OPLS-DA utilizes supervised pattern recognition and effectively filters out irrelevant orthogonal signals. The OPLS-DA score plot exhibited similar overall trends to those seen in the PCA model but with more distinct separation between LT and HT. This analysis further confirmed a clear differentiation between the two temperature conditions (Fig.3b). To identify metabolites that

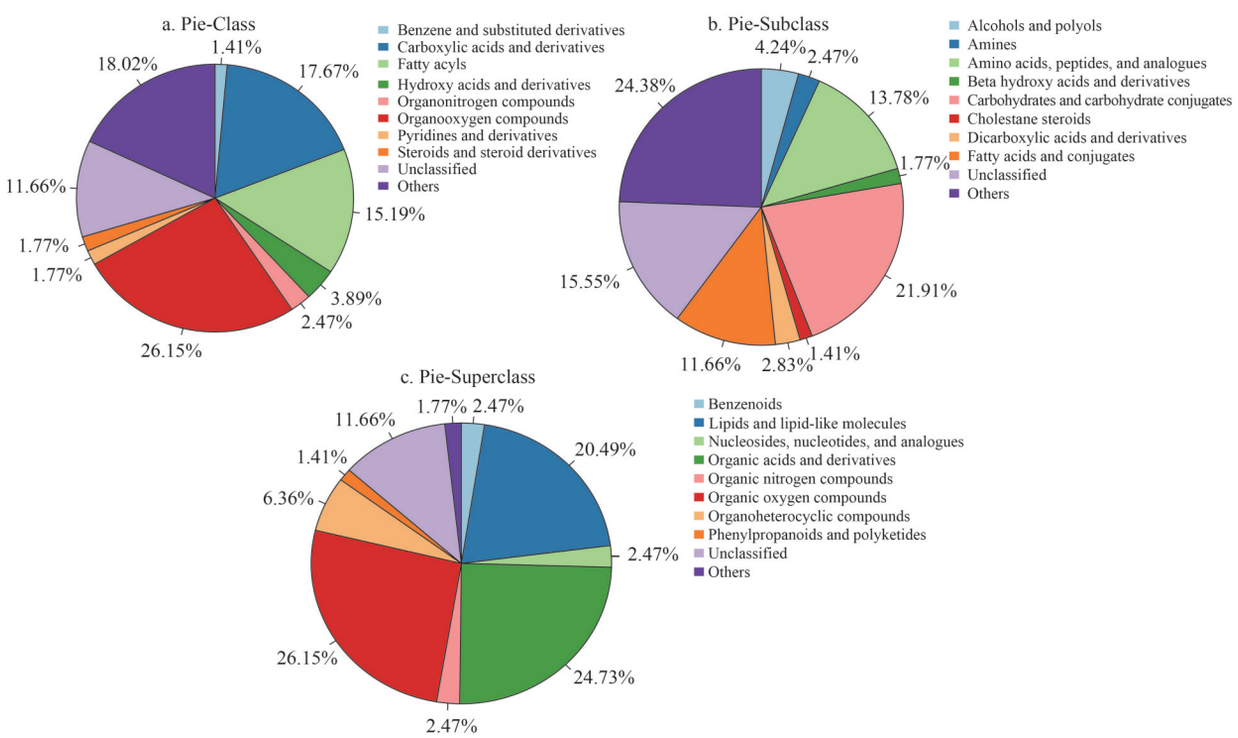

Fig.2 Pie distribution of metabolites

a. represent Pie-Class separation of metabolites; b. Pie-Subclass; c. Pie-Superclass distribution of all metabolites. Different metabolites were separated by different classes shown in different colors.

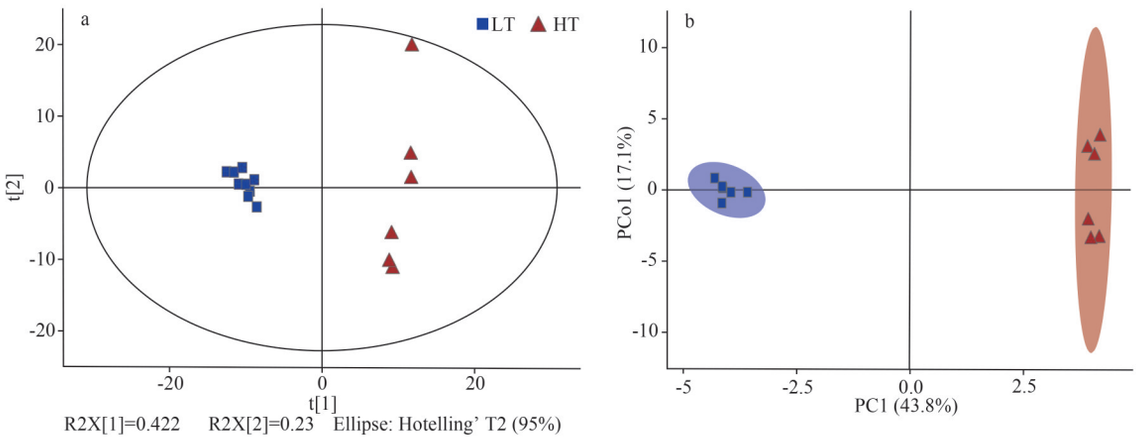

Fig.3 PCA (a) and OPLS-DA analysis (b) for detected compounds in low temperature LT (5 °C) and high temperature HT (25 °C) samples

Data were transformed by $\log_{10}$. Different temperature groups are indicated by the color (red color represents HT (25 °C) samples and blue color represents LT (5 °C) samples). Data presented are from three replicates with three individual experimental repeats.

exhibited significant differences between pairs of *P. yezoensis* samples, pairwise comparisons were conducted using the OPLS-DA model. The OPLS-DA loading plot depicted noticeable distinctions in the metabolome across the samples (Fig.4a). Assessing the parameters of the OPLS-DA models enabled an evaluation of the model's fitting quality and its predictive capability.

The evaluation of all models indicated a satisfactory fit with high predictive power values, as evidenced by all R2Y and Q2 values exceeding 0.8. To validate the models, permutation tests were conducted. The low Q2 intercept values suggested the robustness of the models, with Q2 intercept values in the permutation plot for the four OPLS-DA models remaining below 0.05 after 200 permutations. This further affirmed the reliability and accuracy of the models in capturing the metabolic differences between the *P. yezoensis* samples (Supplementary Fig.S1).

After model diagnosis, S-plot analyses allowed us to identify metabolites that were significantly regulated among the samples as shown in Fig.4b. In the pairwise comparison between HT and LT samples, 60 metabolites were found significantly up-regulated, while 21 etabolites were down-regulated (Supplementary Table S1). Interestingly, the samples maintained at a high temperature of 25 °C exhibited more noticeable changes in metabolite levels. These findings suggest that the distinction between the two groups is substantial and trustworthy, underscoring the significance and reliability of the observed metabolic differences.

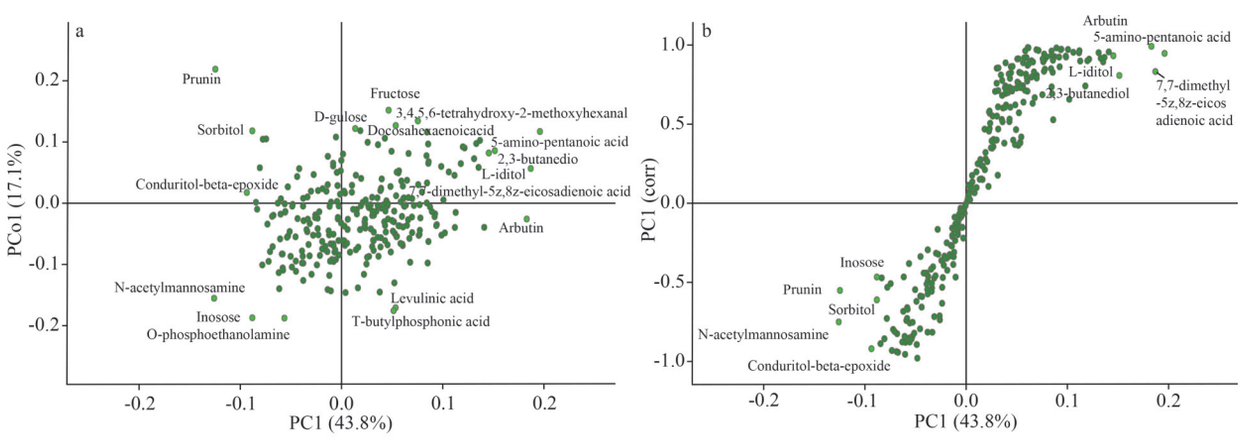

Fig.4 OPLS-DA loadings and S-plots

a. OPLS-DA loadings plot representing the weights of the relative metabolites derived from OPLS-DA model of low temperature and high temperature samples; b. in S-plot the metabolites closer to the upper right and lower left corners indicate a more significant difference.

3.3 Specific change of metabolites in LT and HT samples

To better illustrate the relationship between samples and the variations in metabolite expression among different samples, we conducted hierarchical clustering on the expressions of all significantly differentiated metabolites, sorted by VIP rankings. This method provided a more intuitive visual representation of the metabolic differences between the samples. The 81 compounds were classified into different groups using the human metabolome database.

These compounds included primary metabolites: lipids and derivatives (9), amino acids and derivatives (11), carbohydrates and derivatives (21), alcohols and polyols (2), amines (1), short-chain hydroxy acids and derivatives (1), pyrimidines and pyrimidine derivatives (1), gamma-keto acids and derivatives (1), non-metal phosphates (1), dicarboxylic acids and derivatives (3), tricarboxylic acids and derivatives (1), miscellaneous metallic oxoanionic compounds (1), carboxylic acids (1); and secondary metabolites: furanones (1), pyrrole carboxylic acids and derivatives (1), phenylpropanoids and polyketides (2), pyridinecarboxylic acids and derivatives (2), beta hydroxy acids and derivatives (1), delta valerolactones (1), medium-chain hydroxy acids and derivatives (2), benzenoids (2), alpha hydroxy acids and derivatives (2), and others (13) (Fig.5; Supplementary Table S3).

A larger number of differentially accumulated metabolites were detected in the HT samples (60) compared to the LT samples (21) (Fig.5a;

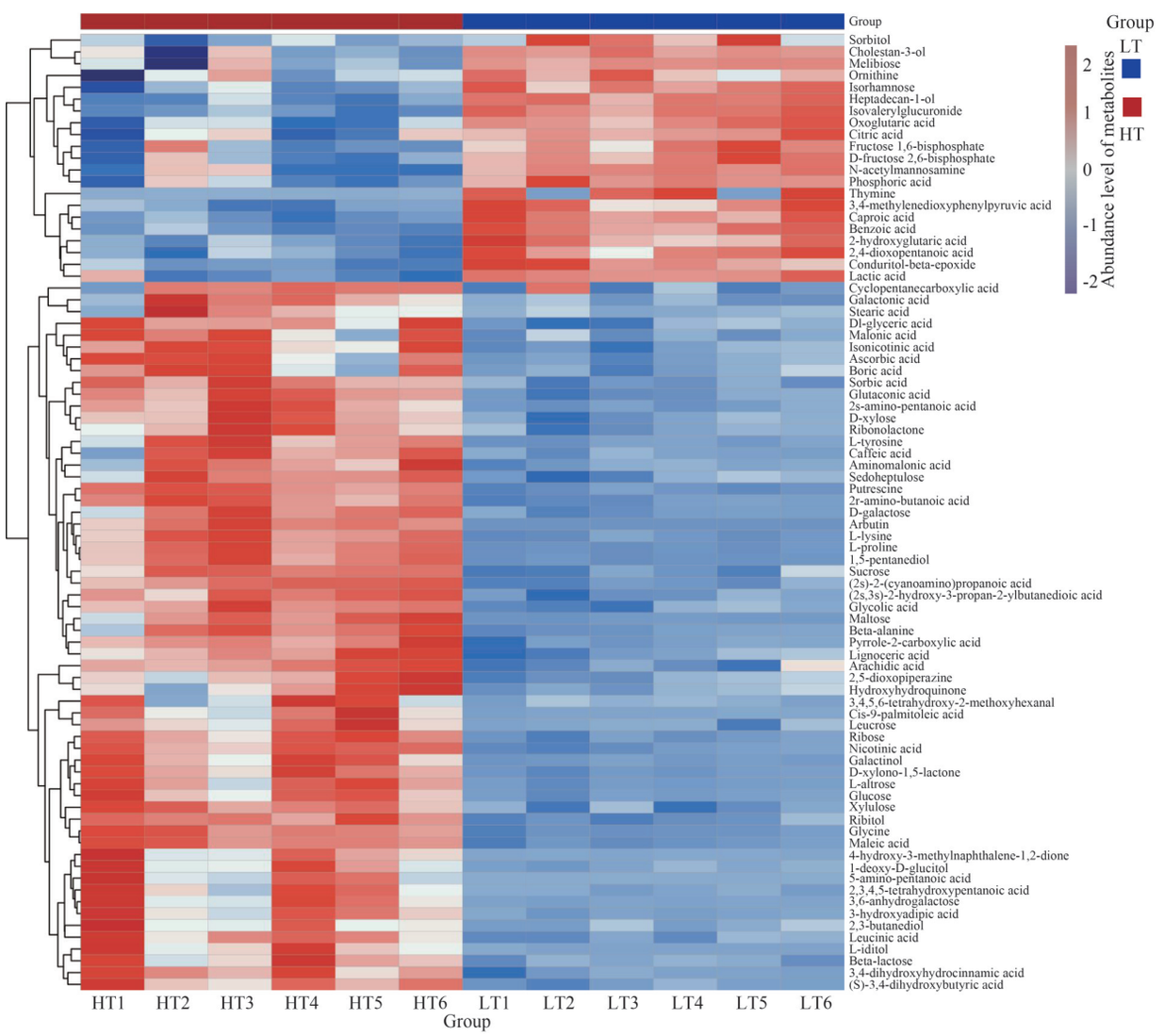

Fig.5 Heatmap analysis of metabolites regulation

The heatmap of 81 compounds of interest and their classification in both LT (5 °C) and HT (25 °C). Red and blue colors represent the increased or reduced accumulation of metabolites, respectively.

Supplementary Fig. S2). Specifically, 60 compounds exhibited significant changes in accumulation and were up-regulated in *P. yezoensis* samples maintained at a high temperature of 25 °C. In contrast, 21 compounds were down-regulated in HT, with significantly higher accumulation observed in samples maintained at LT. At high temperatures, multiple metabolites were found to be up-regulated, suggesting that *P. yezoensis* utilized these compounds for defensive purposes in response to harsh environmental conditions.

A volcano diagram analysis was conducted to assess the number of compounds that exhibited significant accumulation or reduction (P<0.05 and $\log_2$(FC) >1 or <1) in *P. yezoensis* samples maintained at HT and LT after 10 d. In most cases, the number of compounds that significantly accumulated was higher than those that reduced in accumulation. In HT samples, a greater number of metabolites that were deferentially changed in relative abundance was observed (60 were accumulated and 21 were reduced in abundance) (Fig.6). This indicated a notable initial response and metabolic alterations in *P. yezoensis* when exposed to high temperatures. The incorporation of VIP values in the volcano map of metabolites displayed metabolites with significant differences, identified through screening, represented by red and blue dots.

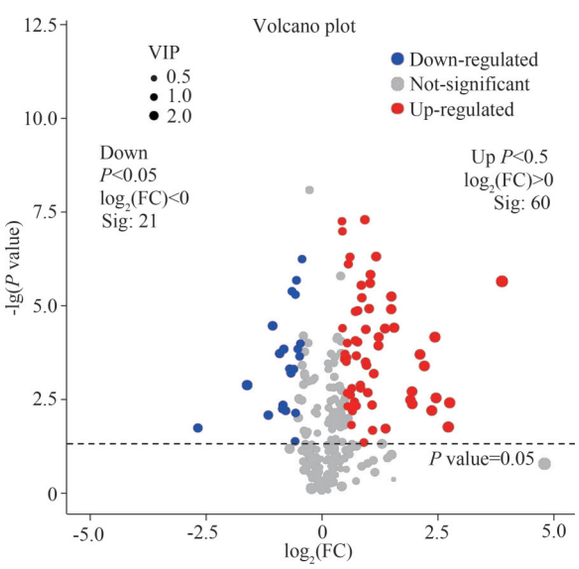

Fig.6 Volcano diagram analysis for metabolites regulation

The abscissa is the $\log_2$(FC) value of the two groups and the ordinate is -lg(P value). Each dot represents a differential metabolite where the red dot is the significantly up-regulated differential metabolite (P<0.05, VIP> 1 and FC>1) in HT group, the blue dot is the significantly down-regulated differential metabolite (P<0.05, VIP>1 and FC<1) in LT group and the gray dots represent the metabolites that were not significantly differentiated.

3.4 Specific change of pathways

The biological pathways significantly impacted by high temperatures were identified using the KEGG database in conjunction with Metaboanalyst 5.0. In Fig.7, the metabolites accumulated in both LT and HT samples from the list of 81 important compounds are shown to have a statistically significant (P<0.05) and high impact on these pathways. The analysis revealed that the ABC transporters, galactose metabolism, and pentose and glucuronate interconversions pathways were prominently up-regulated in *P. yezoensis* samples exposed to high temperatures.

Subsequently, the KEGG pathway database was utilized to identify the relationships among compounds within these metabolic pathways. We identified that 41 out of the 81 compounds were associated with different metabolic pathways within the KEGG database (Supplementary Table S3). The common pathways observed in both up-regulated and down-regulated metabolites were ABC transporters and Galactose metabolism. Most of the metabolites in the ABC transporters, such as maltose, l-lysine, d-xylose, sucrose, putrescine, and glucose were strongly accumulated while sorbitol, melibiose and phosphoric acid were down-regulated in high temperature samples. Similarly, the metabolites in galactose metabolism, such as D-galactose, sucrose, glucose and galactonic acid were up-regulated while sorbitol and melibiose were down-regulated in treated samples. Apart from the ABC transporters and galactose metabolism, the metabolites belonging to other pathways also showed up-regulation and down-regulation due to high temperature. In addition, the up-regulated metabolites belonging to glycolysis/gluconeogenesis were arbutin and glucose while fructose 1,6-bisphosphate down-regulated in treated samples.

A z-score plot clearly represented the regulation of the top 20 metabolites between low and high temperature samples (Supplementary Fig.S3). The metabolites of different pathways showed either accumulation or reduction, indicating a complex regulatory system in response to high temperature. In ABC transporter the metabolites putrescine, maltose, D-xylose, glucose, L-lysine were up-regulated in HT samples while down-regulated in LT and metabolites sorbitol, melibiose were down-regulated in HT samples while up-regulated in LT (Fig.8a & b). In galactose metabolism the metabolites, D-galactose, D-galactonate, glucose, sucrose were up-regulated in HT samples while

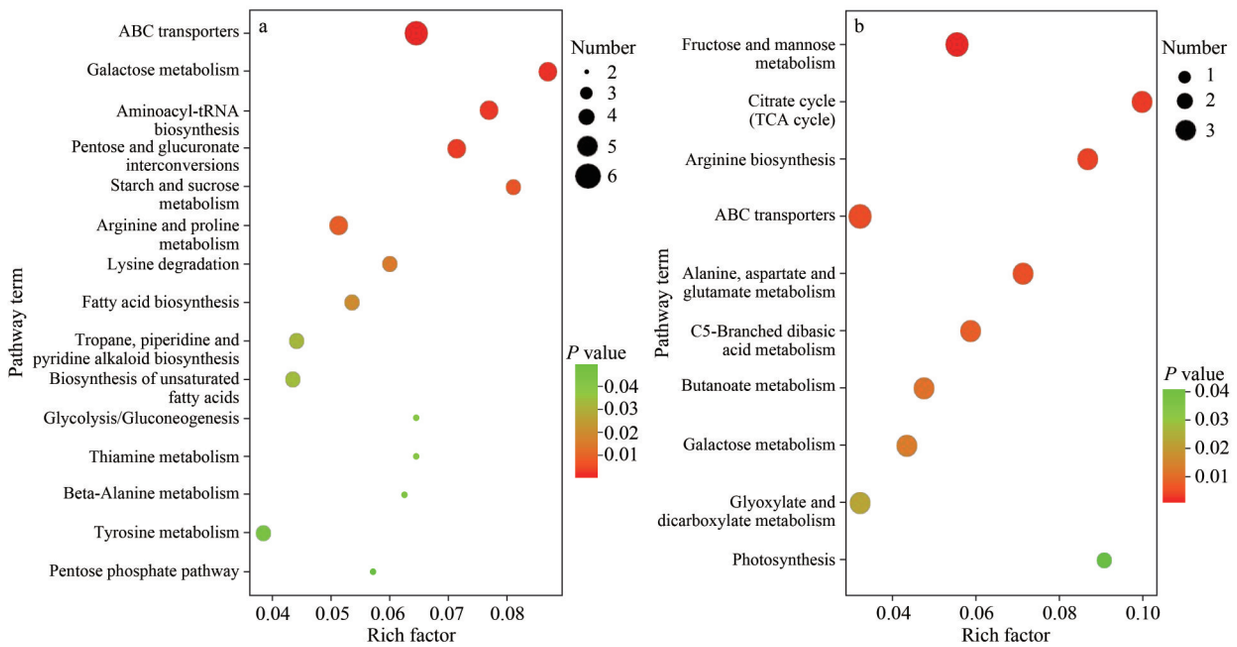

Fig.7 Metabolites pathways

a. significant enrichment pathway analysis of metabolites that showed up-regulation; b. the pathways that were down-regulated in the samples. The *y*-axis (-lg(*P*)) indicates the *P* value of the pathway enrichment analysis, represented by the bubble colors (darker color means more significant enrichment). The *x*-axis is the impact factor of topological analysis, represented by the bubble sizes (bigger bubble means a higher impact).

down-regulated in LT and metabolites sorbitol, melibiose were down-regulated in HT samples while up-regulated in LT (Fig.9a & b).

4 DISCUSSION

Pyropia yezoensis, commonly known as nori, is a red alga that plays a vital role for its nutritional benefits and distinctive flavor in the industries of food (Murayama et al., 2020). The presence of metabolites in *P. yezoensis* is responsible for its bioactive properties and sensory attributes, making it a desirable ingredient in diverse culinary applications (Pereira, 2023). It is crucial to understand the composition and regulation of these metabolites in order to fully harness the potential benefits of *P. yezoensis* (de Sousa Santos Hempel et al., 2023; Patwary, 2023).

The non-targeted metabolomic analysis carried out in this study using GC-MS provided in-depth insights into the wide array of metabolites present in *P. yezoensis*. The analysis revealed a complex metabolite profile, encompassing various chemical classes like lipids, amino acids, carbohydrates, and secondary metabolites. This comprehensive profiling identified several bioactive compounds, including alcohol and polyols, amines, amino acids-peptides-analogues, beta hydroxy acids and derivatives, carbohydrates and carbohydrate conjugates, cholestane steroids, dicarboxylic acid and derivatives, fatty acids and conjugates, which contribute to the nutritional and functional properties of *P. yezoensis*.

In a recent study conducted by Iizasa et al. (2023), the importance of lipid content in *P. yezoensis* was highlighted and it was suggested that the fatty liver condition caused by obesity could be alleviated through the use of susabinori lipids (SNL) rich in eicosapentaenoic acid (EPA). Our findings also showed that lipid accumulation in HT samples was higher than LT, underscoring the nutritional and pharmaceutical value of *P. yezoensis* when expose to high temperature.

According to different literatures, *P. yezoensis* having economic importance primarily cultivated in East Asian countries, typically grows in temperatures lower than 18 °C. However, several mutant strains of *P. yezoensis* with high temperature tolerance have been developed, enabling it to thrive in conditions exceeding 20 °C. The fluctuation in temperature, specifically raised temperatures from 18 °C to 23 °C and 24 °C, has been shown to prevent the development of *P. yezoensis* germlings and lead to decomposition of distributed blades, resulting in a significant decrease in production (Zhang et al., 2011; Ding et al., 2016; Shin et al., 2018). This study also examined the effects of high

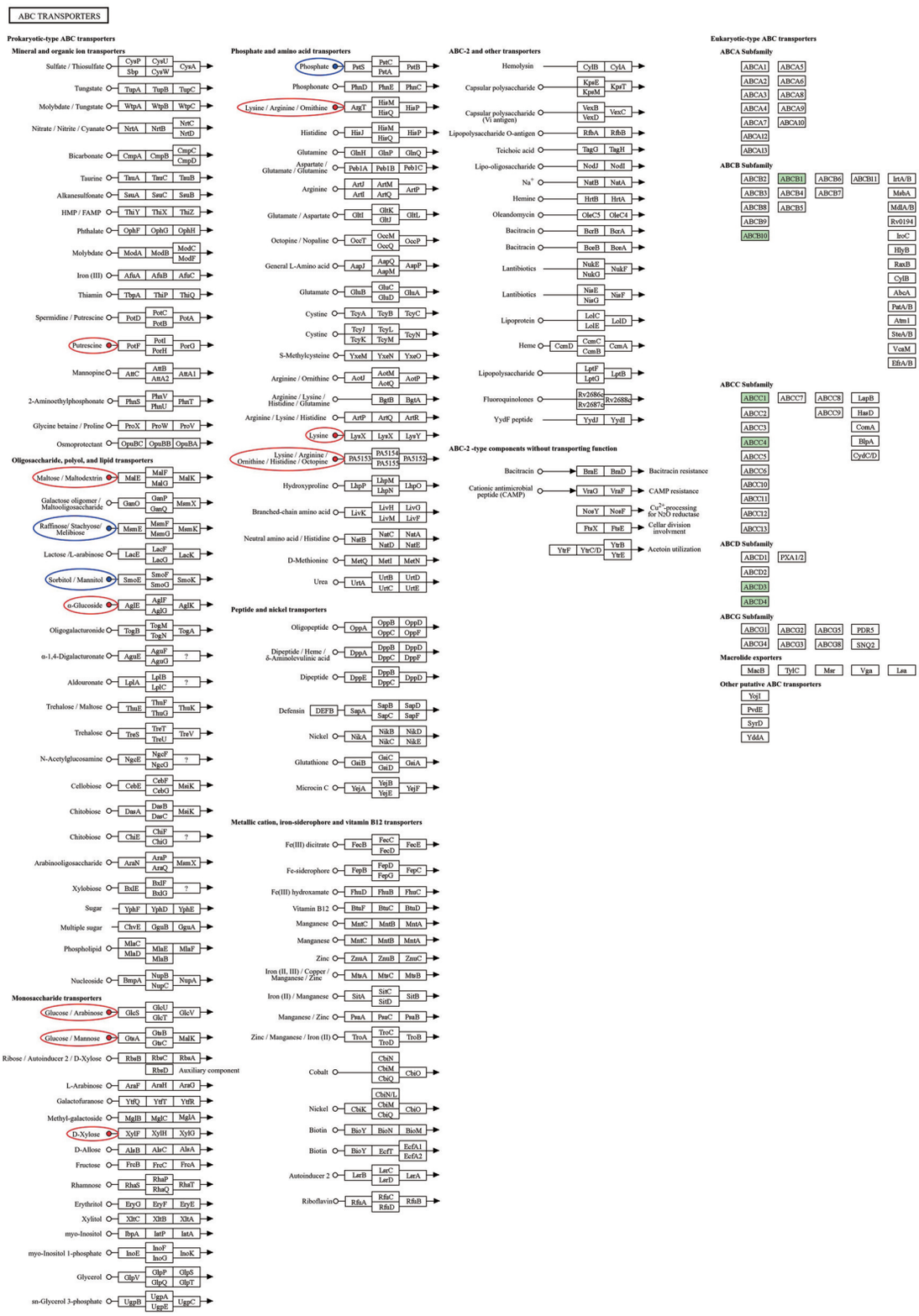

Fig.8 ABC transporter

a. regulation of different metabolites were observed in ABC transporter. The differential metabolic pathways were visualized using the KEGG pathway mapper function, with the differential metabolites colored and displayed based on their up- and down-regulation status. In the pathway diagram, small circles represent metabolites, with up-regulated metabolites shown in red and down-regulated metabolites in blue; b. the regulated metabolites from ABC transporter were separately represented from both samples groups. Red indicates the high temperature samples while blue shows low temperature samples.

To be continued

Fig.8 Continued

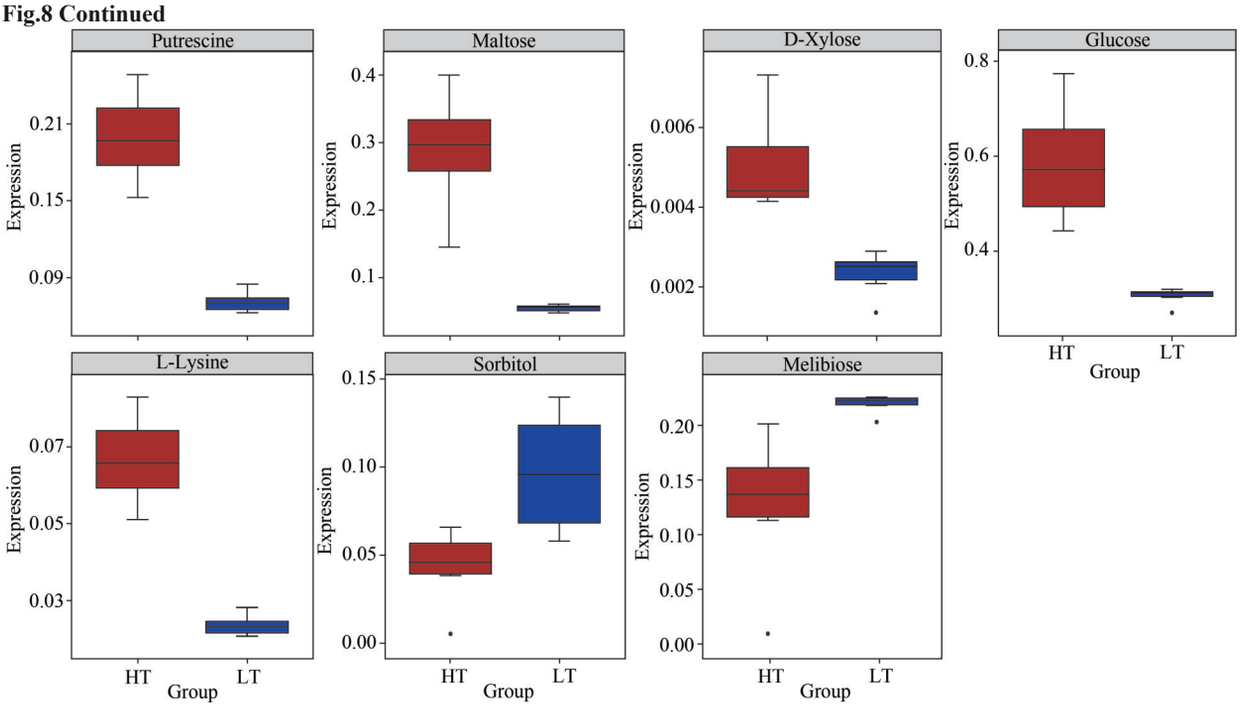

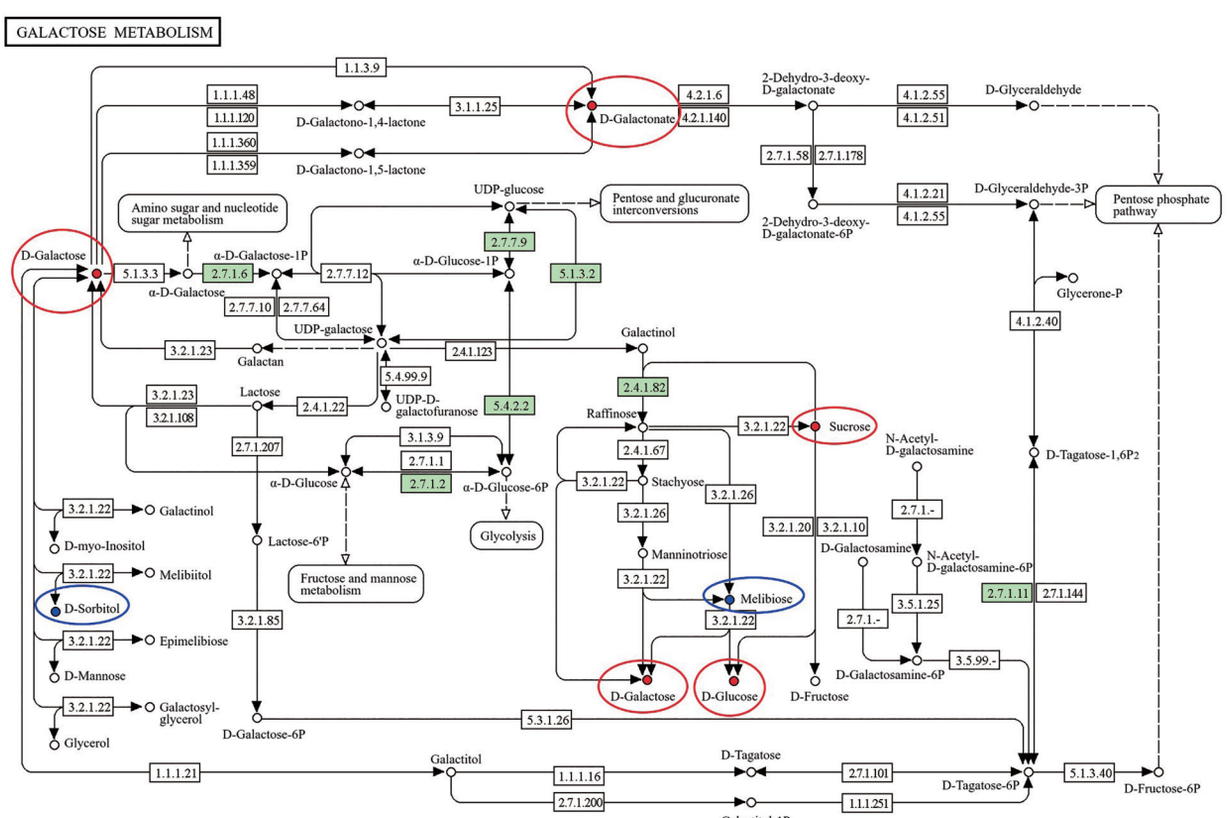

Fig.9 Galactose metabolism

a. regulation of different metabolites were observed in Galactose metabolism. The differential metabolic pathways were visualized using the KEGG pathway mapper function, with the differential metabolites colored and displayed based on their up- and down-regulation status. In the pathway diagram, small circles represent metabolites, with up-regulated metabolites shown in red and down-regulated metabolites in blue; b. the regulated metabolites from Galactose metabolism were separately represented from both samples groups. Red indicates the high temperature samples while blue shows low temperature samples.

To be continued

Fig.9 Continued

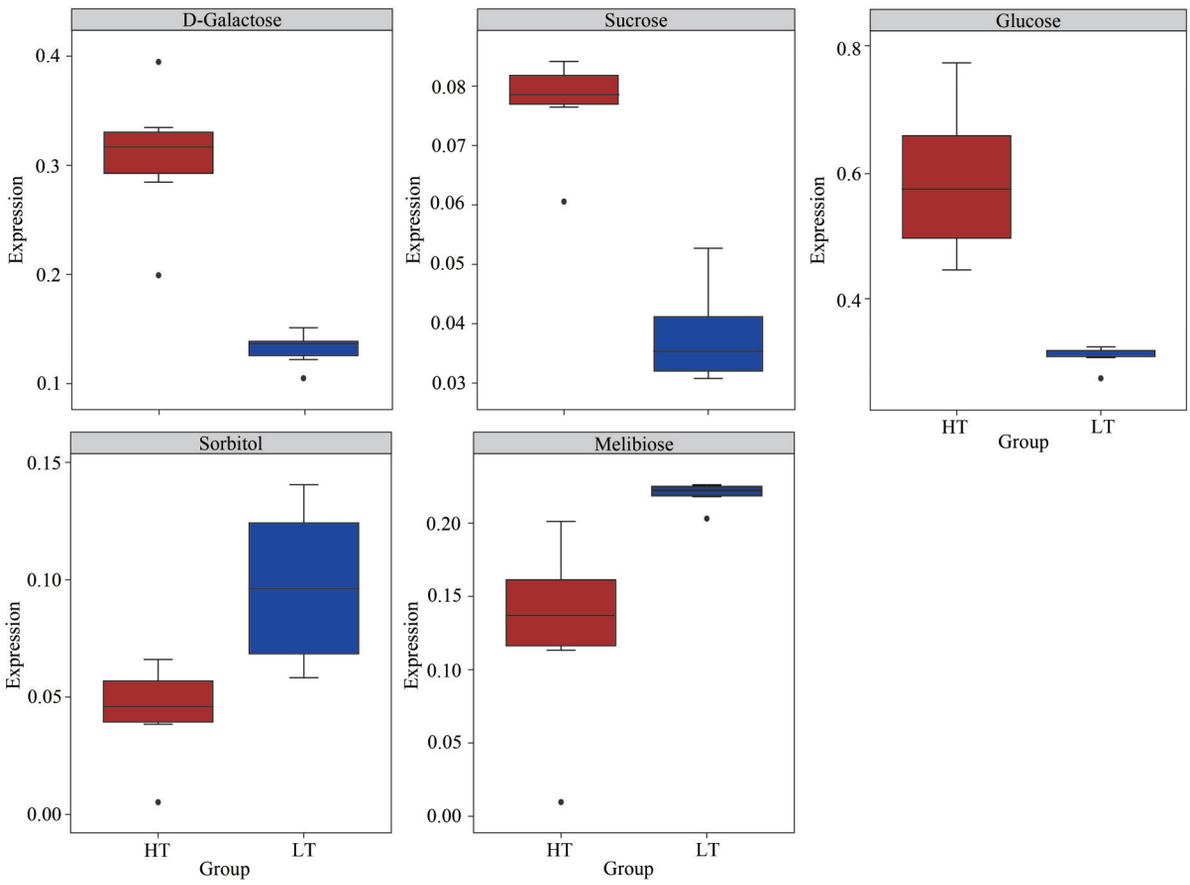

temperature stress but the focus was to investigate the regulation of metabolites in *P. yezoensis* when the temperature exceeds than normal. According to the cloning and transcriptomic analyses of (Chen et al., 2015), the degrading impacts of abiotic factors (high temperature) determined sHSPs (small heat-shock proteins) synthesis in *Pyropia*. High temperature stress has been found to trigger changes in the levels of different metabolites, suggesting a potential response and adaptation mechanism of *P. yezoensis* to stressful environmental conditions. Our findings revealed that some metabolites decreased in concentration while many of them increased in response to high temperature stress.

The recent research of temperature stress on another red algae *P. haitanensis* energy metabolism, revealed significant expression of its associated genes that enhance carbohydrate metabolism (Wang et al., 2018). The citrate cycle, responsible for oxidizing respiratory substrates to drive ATP synthesis, has a substantial impact on a plant's ability to resist abiotic stresses (Mailloux et al., 2007; Sweetlove et al., 2010). As different compounds and secondary metabolites and their respective pathways were up-regulated in HT samples of *P. yezoensis* in our study suggests the defensive mechanism of this algae against abiotic temperature stress.

The previous studies highlighted that over-expression of ABC transporter and their respective genes involved in the response of different environmental stresses (Chen et al., 2018; Dahuja et al., 2021). The tolerance of *U. prolifera* to temperature stress revealed that the metabolic shifts involved in the pathways of galactose metabolism, starch/sucrose, and alanine/aspartate/glutamate respectively (He et al., 2018). In this study, different pathways up- and down-regulation were highlighted in response of HT and LT temperature in which ABC transporters and Galactose metabolism were the common pathways (Fig.7). These findings have important implications as they offer valuable insights into the biochemical pathways and adaptive responses of *P. yezoensis*, revealing how this alga is able to cope with environmental stress. Understanding the metabolite composition and regulatory mechanisms in *P. yezoensis* for high temperature conditions response. These practices can provide valuable insights for the development of strategies aimed at

enhancing its cultivation and utilization in variable environmental stress. This knowledge can be harnessed to optimize the production processes of *P. yezoensis* while assure its nutritional quality and functional characteristics.

This research enhances the current understanding of the metabolomics of *P. yezoensis* and underscores the significance of environmental variables in comprehending the bioactivity and adaptability of this valuable red alga. Subsequent investigations in this field may give rise to novel strategies for improving the cultivation, nutritional content, and functional characteristics of *P. yezoensis*, thereby offering advantages to both the food industry and consumers.

5 CONCLUSION

In conclusion, our study uncovered the diverse range of metabolites present in *Pyropia yezoensis* and their dynamic response to high temperature stress. Through advanced analytical techniques and statistical analysis, we discovered various metabolites that perform a critical role in *P. yezoensis'* adaptation to high temperature. The significant differences in metabolite profiles between HT and LT samples emphasize the profound impact of high temperature on biochemical composition and up-regulation of various metabolites in *P. yezoensis*. Our findings revealed the activation of key biochemical pathways and adaptive responses in *P. yezoensis* under high temperature conditions, providing valuable insights into its growth and development. Highlighting the complex interaction between *P. yezoensis* and its environment, this study revealed insights to exploit the biochemical diversity of *P. yezoensis* when expose to high temperature conditions. The study revealed that *Pyropia yezoensis* contains different nutritional components regulated by high temperature. Research on the mutant development of *P. yezoensis* holds prospect for enhancing traits related to stress tolerance, growth rate, nutritional values, and yield in this valuable seaweed species.

6 DATA AVAILABILITY STATEMENT

The data that support the findings of this study are openly available from the corresponding author upon reasonable request.

7 ACKNOWLEDGMENT

The authors acknowledge with gratitude, the efforts and contributions of Shanghai OE Biotech. Co., Ltd., China

References

Aliferis K A, Cubeta M A, Jabaji S. 2013. Chemotaxonomy of fungi in the *Rhizoctonia solani* species complex performing GC/MS metabolite profiling. *Metabolomics*, **9**(S1): 159-169, https://doi.org/10.1007/s11306-011-0340-1.

Barange M. 2018. Fishery and Aquaculture Statistics. FAO Yearbook. Fishery and Aquaculture Statistics, I-82.

Chen N M, Song B, Tang S et al. 2018. Overexpression of the ABC transporter gene *TsABCG11* increases cuticle lipids and abiotic stress tolerance in *Arabidopsis*. *Plant Biotechnology Reports*, **12**(5): 303-313, https://doi.org/10.1007/s11816-018-0495-6.

Chen Y T, Xu Y, Ji D H et al. 2015. Cloning and expression analysis of two small heat shock protein (sHsp) genes from *Pyropia haitanensis*. *Journal of Fisheries of China*, **39**(2): 182-192, https://doi.org/10.3724/SP.J.1231.2015.59419. (in Chinese with English abstract)

Choi J W, Kim Y M, Park S J et al. 2015. Protective effect of *Porphyra yezoensis* glycoprotein on D-galactosamine-induced cytotoxicity in Hepa 1c1c7 cells. *Molecular Medicine Reports*, **11**(5): 3914-3919, https://doi.org/10.3892/mmr.2015.3244.

Choi S, Hwang M S, Im S et al. 2013. Transcriptome sequencing and comparative analysis of the gametophyte thalli of *Pyropia tenera* under normal and high temperature conditions. *Journal of Applied Phycology*, **25**(4): 1237-1246, https://doi.org/10.1007/s10811-012-9921-2.

Dahuja A, Kumar R R, Sakhare A et al. 2021. Role of ATP-binding cassette transporters in maintaining plant homeostasis under abiotic and biotic stresses. *Physiologia Plantarum*, **171**(4): 785-801, https://doi.org/10.1111/ppl.13302.

de Sousa Santos Hempel M, Colepicolo P, Zambotti-Villela L. 2023. Macroalgae biorefinery for the cosmetic industry: basic concept, green technology, and safety guidelines. *Phycology*, **3**(1): 211-241, https://doi.org/10.3390/phycology3010014.

Ding H C, Zhang B L, Yan X H. 2016. Isolation and characterization of a heat-resistant strain with high yield of *Pyropia yezoensis* Ueda (Bangiales, Rhodophyta). *Aquaculture and Fisheries*, **1**: 24-33, https://doi.org/10.1016/j.aaf.2016.09.001.

Eitsuka T, Nakagawa K, Igarashi M et al. 2004. Telomerase inhibition by sulfoquinovosyldiacylglycerol from edible purple laver (*Porphyra yezoensis*). *Cancer Letters*, **212**(1): 15-20, https://doi.org/10.1016/j.canlet.2004.03.019.

He Y L, Hu C Y, Wang Y H et al. 2018. The metabolic survival strategy of marine macroalga *Ulva prolifera* under temperature stress. *Journal of Applied Phycology*, **30**(6): 3611-3621, https://doi.org/10.1007/s10811-018-1493-3.

Hirano Y, Hattori M, Takahashi K. 2005. Interaction of porphyran with a hydrophobic surface and stabilization of liposomes. *Journal of Agricultural and Food Chemistry*,

53(25): 9800-9804, https://doi.org/10.1021/jf050793e.

Hwang H J, Kwon M J, Kim I H et al. 2008. Chemoprotective effects of a protein from the red algae *Porphyra yezoensis* on acetaminophen-induced liver injury in rats. *Phytotherapy Research*, **22**(9): 1149-1153, https://doi.org/10.1002/ptr.2368.

Iizasa S, Nagao K, Tsuge K et al. 2023. Identification of genes regulated by lipids from seaweed Susabinori (*Pyropia yezoensis*) involved in the improvement of hepatic steatosis: Insights from RNA-Seq analysis in obese *db*/*db* mice. *PLoS One*, **18**(12): e0295591, https://doi.org/10.1371/journal.pone.0295591.

Isaka S, Cho K, Nakazono S et al. 2015. Antioxidant and anti-inflammatory activities of porphyran isolated from discolored nori (*Porphyra yezoensis*). *International Journal of Biological Macromolecules*, **74**: 68-75, https://doi.org/10.1016/j.ijbiomac.2014.11.043.

Kanehisa M, Goto S. 2000. KEGG: Kyoto encyclopedia of genes and genomes. *Nucleic Acids Research*, **28**(1): 27-30, https://doi.org/10.1093/nar/28.1.27.

Kayama M, Iijima N, Kuwahara M et al. 1985. Effect of water temperature on the fatty acid composition of *Porphyra*. *Bulletin of the Japanese Society of Scientific Fisheries*, **51**(4): 687, https://doi.org/10.2331/suisan.51.687.

Kientz B, Thabard M, Cragg S M et al. 2011. A new method for removing microflora from macroalgal surfaces: an important step for natural product discovery. *Botanica Marina*, **54**(5): 457-469, https://doi.org/10.1515/BOT.2011.053.

Kumar Y, Tarafdar A, Badgujar P C. 2021. Seaweed as a source of natural antioxidants: therapeutic activity and food applications. *Journal of Food Quality*, **2021**: 1-17, https://doi.org/10.1155/2021/5753391.

Larcher W. 2003. Physiological Plant Ecology: Ecophysiology and Stress Physiology of Functional Groups. 4th edn. Springer, Berlin Heidelberg.

Mailloux R J, Bériault R, Lemire J et al. 2007. The tricarboxylic acid cycle, an ancient metabolic network with a novel twist. *PLoS One*, **2**(8): e690, https://doi.org/10.1371/journal.pone.0000690.

Mastrangelo A, Ferrarini A, Rey-Stolle F et al. 2015. From sample treatment to biomarker discovery: a tutorial for untargeted metabolomics based on GC-(EI)-Q-MS. *Analytica Chimica Acta*, **900**: 21-35, https://doi.org/10.1016/j.aca.2015.10.001.

Miyamoto E, Yabuta Y, Kwak C S et al. 2009. Characterization of vitamin B_{12} compounds from Korean purple laver (*Porphyra* sp.) products. *Journal of Agricultural and Food Chemistry*, **57**(7): 2793-2796, https://doi.org/10.1021/jf803755s.

Mohamed S, Hashim S N, Rahman H A. 2012. Seaweeds: a sustainable functional food for complementary and alternative therapy. *Trends in Food Science & Technology*, **23**(2): 83-96, https://doi.org/10.1016/j.tifs.2011.09.001.

Murayama F, Kusaka K, Uchida M et al. 2020. Preparation of nori *Pyropia yezoensis* enriched with free amino acids by aging the culture with *nori koji*. *Fisheries Science*, **86**(3): 531-542, https://doi.org/10.1007/s12562-020-01419-z.

Niwa K. 2010. Genetic analysis of artificial green and red mutants of *Porphyra yezoensis* Ueda (Bangiales, Rhodophyta). *Aquaculture*, **308**(1-2): 6-12, https://doi.org/10.1016/j.aquaculture.2010.08.007.

Niwa K, Furuita H, Aruga Y. 2003. Free amino acid contents of the gametophytic blades from the green mutant conchocelis and the heterozygous conchocelis in *Porphyra yezoensis* Ueda (Bangiales, Rhodophyta). *Journal of Applied Phycology*, **15**(5): 407-413, https://doi.org/10.1023/A:1026087316190.

Niwa K, Furuita H, Yamamoto T. 2008. Changes of growth characteristics and free amino acid content of cultivated *Porphyra yezoensis* Ueda (Bangiales Rhodophyta) blades with the progression of the number of harvests in a nori farm. *Journal of Applied Phycology*, **20**(5): 687-693, https://doi.org/10.1007/s10811-007-9273-5.

Noda H. 1993. Health benefits and nutritional properties of nori. *Journal of Applied Phycology*, **5**(2): 255-258, https://doi.org/10.1007/BF00004027.

Park S E, Seo S H, Lee K I et al. 2018. Metabolite profiling of fermented ginseng extracts by gas chromatography mass spectrometry. *Journal of Ginseng Research*, **42**(1): 57-67, https://doi.org/10.1016/j.jgr.2016.12.010.

Patwary Z P. 2023. Multi-Omics Investigation Across the life-History Stages of the Red Seaweed, *Asparagopsis taxiformis*. University of the Sunshine Coast, Queensland, https://doi.org/10.25907/00757.

Pereira L. 2023. Atlantic algae as food and their extracts. *Exploration of Foods and Foodomics*, **1**: 15-31, https://doi.org/10.37349/eff.2023.00003.

Qu W J, Ma H L, Pan Z L et al. 2010. Preparation and antihypertensive activity of peptides from *Porphyra yezoensis*. *Food Chemistry*, **123**(1): 14-20, https://doi.org/10.1016/j.foodchem.2010.03.091.

Sahoo D, Tang X R, Yarish C. 2002. *Porphyra*—the economic seaweed as a new experimental system. *Current Science*, **83**(11): 1313-1316.

Shin E S, Hwang H J, Kim I H et al. 2011. A glycoprotein from *Porphyra yezoensis* produces anti-inflammatory effects in liposaccharide-stimulated macrophages via the TLR4 signaling pathway. *International Journal of Molecular Medicine*, **28**(5): 809-815, https://doi.org/10.3892/ijmm.2011.729.

Shin Y J, Min S R, Kang D Y et al. 2018. Characterization of high temperature-tolerant strains of *Pyropia yezoensis*. *Plant Biotechnology Reports*, **12**(5): 365-373, https://doi.org/10.1007/s11816-018-0499-2.

Sutherland J E, Lindstrom S C, Nelson W A et al. 2011. A new look at an ancient order: generic revision of the Bangiales (Rhodophyta). *Journal of Phycology*, **47**(5): 1131-1151, https://doi.org/10.1111/j.1529-8817.2011.01052.x.

Sweetlove L J, Beard K F M, Nunes-Nesi A et al. 2010. Not just a circle: flux modes in the plant TCA cycle. *Trends in Plant Science*, **15**(8): 462-470, https://doi.org/10.1016/j.tplants.2010.05.006.

Takahashi K, Hirano Y, Araki S et al. 2000. Emulsifying ability of porphyran prepared from dried nori,

Porphyrayezoensis, a red alga. *Journal of Agricultural and Food Chemistry*, **48**(7): 2721-2725, https://doi.org/10.1021/jf990990b.

Toyosaki T, Iwabuchi M. 2009. New antioxidant protein in seaweed (*Porphyra yezoensis Ueda*). *International Journal of Food Sciences and Nutrition*, **60**(S2): 46-56, https://doi.org/10.1080/09637480802345591.

Wang W L, Teng F, Lin Y H et al. 2018. Transcriptomic study to understand thermal adaptation in a high temperature-tolerant strain of *Pyropia haitanensis*. *PLoS One*, **13**(4): e0195842, https://doi.org/10.1371/journal.pone.0195842.

Wheelock Å M, Wheelock C E. 2013. Trials and tribulations of 'omics data analysis: assessing quality of SIMCA-based multivariate models using examples from pulmonary medicine. *Molecular BioSystems*, **9**(11): 2589-2596, https://doi.org/10.1039/c3mb70194h.

Xu Y, Chen C S, Ji D H et al. 2014. Proteomic profile analysis of *Pyropia haitanensis* in response to high-temperature stress. *Journal of Applied Phycology*, **26**(1): 607-618, https://doi.org/10.1007/s10811-013-0066-8.

Zhang B L, Yan X H, Huang L B. 2011. Evaluation of an improved strain of *Porphyra yezoensis* Ueda (Bangiales, Rhodophyta) with high-temperature tolerance. *Journal of Applied Phycology*, **23**(5): 841-847, https://doi.org/10.1007/s10811-010-9587-6.

Zhang W Y, Chen H, Wang S J et al. 2001. An acidic polysaccharide with xylose branches from *Porphyra yezoensis*. *Chinese Science Bulletin*, **46**(3): 207-210, https://doi.org/10.1007/BF03187168.

Zhao L J, Zhang H L, White J C et al. 2019. Metabolomics reveals that engineered nanomaterial exposure in soil alters both soil rhizosphere metabolite profiles and maize metabolic pathways. *Environmental Science*: *Nano*, **6**(6): 1716-1727, https://doi.org/10.1039/C9EN00137A.

Zhou C S, Ma H L. 2006. Ultrasonic degradation of polysaccharide from a red algae (*Porphyra yezoensis*). *Journal of Agricultural and Food Chemistry*, **54**(6): 2223-2228, https://doi.org/10.1021/jf052763h.

Electronic supplementary material

Supplementary material (Supplementary Tables S1–S3 and Figs.S1–S3) is available in the online version of this article at https://doi.org/10.1007/s00343-024-4081-1.